Nanoscale

PAPER

Dependence of coupling of quasi 2-D MoS_2 with substrates on substrate types, probed by temperature dependent Raman scattering†

Cite this: *Nanoscale*, 2014, **6**, 4920

Liqin Su,[a] Yong Zhang,*[a] Yifei Yu[b] and Linyou Cao[b]

Received 5th December 2013
Accepted 3rd February 2014

DOI: 10.1039/c3nr06462j

www.rsc.org/nanoscale

This work reports a study on the temperature dependence of in-plane E^1_{2g} and out-of-plane A_{1g} Raman modes of single-layer (1L) and bi-layer (2L) MoS_2 films on sapphire (epitaxial) and SiO_2 (transferred) substrates as well as bulk MoS_2 single crystals in a temperature range of 25–500 °C. For the films on the transferred SiO_2 substrate, the in-plane E^1_{2g} mode is only weakly affected by the substrate, whereas the out-of-plane A_{1g} mode is strongly perturbed, showing highly nonlinear, sometimes even non-monotonic, temperature dependence on the Raman peak shift and linewidth. In contrast, for the films on the epitaxial sapphire substrate, E^1_{2g} is affected more significantly by the substrate than A_{1g}. This study suggests that the 2-D film–substrate coupling depends sensitively on the preparation method, and in particular on the film morphology for the transferred film. These findings are vitally important for the fundamental understanding and application of this quasi 2-D material that is expected to be supported by a substrate in most circumstances.

Introduction

Two-dimensional (2-D) materials such as graphene and hexagonal boron nitride (h-BN) have attracted a tremendous amount of attention because of their extraordinary physical properties.[1–6] However, graphene is a zero band gap material with vanishing density of states at the Dirac point, making it difficult to be used in electronic devices, particularly in transistors.[7] Although several strategies of band gap engineering have been applied to open the band gap, generating a band gap larger than 400 meV remains a challenge.[8–10] In contrast, h-BN has a band gap of 5.2 eV, too large for an efficient performance in electronic devices.[11] Recently, single-layer molybdenum disulfide (MoS_2), consisting of three atomic layers of one Mo and two S, has been shown to exhibit a direct band gap of ~1.8 eV, while bulk MoS_2 has an indirect band gap of 1.29 eV.[12,13] Since single-layer MoS_2 shares a number of common properties with graphene such as a 2-D layered structure but has a finite band gap, it is considered to be an alternative to graphene, attracting significant research interest. By using the mechanical exfoliation method, single- and few-layer MoS_2 samples have been obtained, showing extremely strong photoluminescence compared to bulk MoS_2. Recently, single-layer MoS_2 based FETs have been reported to have a mobility of at least 200 $cm^2\ V^{-1}\ s^{-1}$ and a current on/off ratio of 1×10^8.[14] These promising optical and electronic properties can potentially lead to the development of high-quality low-power optoelectronic devices. Synthesis of a large area of MoS_2 atomic layers has been demonstrated using a vapor-phase deposition method.[15] Recently, it has been reported that a self-limiting approach can produce thin MoS_2 films over an area of centimeters with the layer number precisely controllable.[16]

A single-layer MoS_2 is formed by the arrangement of a triangular or simple hexagonal plane of Mo atoms sandwiched between two triangular layers of S atoms in a triangular prismatic fashion (see Fig. 1(a)). Bulk MoS_2 is a periodically stacked S–Mo–S layers through the van der Waals force. The space group of single layer MoS_2 is $P6m2$ (point group D_{3h}), and the four first-order Raman active modes at the center of the Brillouin zone are 32 cm^{-1} (E^2_{2g}), 286 cm^{-1} (E_{1g}), 383 cm^{-1} (E^1_{2g}), and 408 cm^{-1} (A_{1g}).[17,18] The E^2_{2g} mode arises from the relative motion between

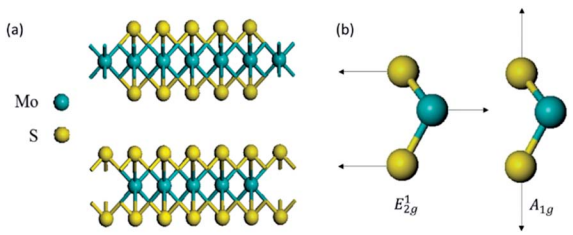

Fig. 1 (a) Schematic model of MoS_2 bulk and single layer. (b) In-plane phonon E^1_{2g} and out-of-plane phonon A_{1g} for single-layer MoS_2.

[a]*Electrical and Computer Engineering Department, University of North Carolina at Charlotte, Charlotte, NC 28223, USA. E-mail: yong.zhang@uncc.edu*

[b]*Department of Materials Science and Engineering, North Carolina State University, Raleigh, NC 27695, USA*

† Electronic supplementary information (ESI) available: The temperature-dependent Raman scattering of another two mechanically exfoliated 1L MoS_2 films on the SiO_2/Si substrate. See DOI: 10.1039/c3nr06462j

two MoS_2 layers, which will vanish in the single layer sample. The E_{1g} mode is forbidden in back-scattering measurement on the basal plane perpendicular to the c axis. The E^1_{2g} mode is attributed to the in-plane relative motion between the two S atoms and the Mo atom, whereas the A_{1g} mode is attributed to the out-of-plane vibration of two S atoms in opposite directions. Strictly speaking, the two active Raman modes E^1_{2g} and A_{1g} (in D_{6h} for bulk MoS_2) should be assigned as E′ and A'_1 in the monolayer MoS_2 (in D_{3h}).[19,20] However, to see the evolution from the bulk to single-layer,[17,21] the two modes are simply labelled as E^1_{2g} and A_{1g} for all cases, as commonly done in the literature. Raman spectroscopy is a sensitive nondestructive technique to investigate structural and electronic properties of MoS_2. Similar to graphene, the Raman peak positions depend on the number of MoS_2 single layers, which makes it possible to determine the number of layers from Raman spectra.[21,22]

In this work, we report on the temperature dependent Raman spectra of both single- (1L) and bi-layer (2L) MoS_2, as well as the bulk sample. The knowledge of temperature dependent vibrational properties is important for further understanding the electron–phonon interaction, transport properties, and crystal structure of materials, which may largely impact the performance of electronic devices. Furthermore, because the MoS_2 is expected to be supported by a substrate in most if not all real applications, thus the coupling with the substrate is inevitable, this temperature dependence study offers valuable insights into the effect of the substrate, which might not be apparent at a fixed temperature. Since SiO_2/Si is widely used as the substrate for fabricating electronic devices after the film being transferred from the original growth substrate, it is of particular interest to investigate the 2-D film with the SiO_2/Si substrate.

The temperature variations of the Raman frequencies in MoS_2 on SiO_2/Si have been studied previously, giving the linear temperature coefficients, respectively, for E^1_{2g} and A_{1g} modes: for few layers, -0.0132 cm^{-1} K^{-1} and -0.0123 cm^{-1} K^{-1} from 83 to 523 K;[23] for a single layer, -0.0179 cm^{-1} K^{-1} and -0.0143 cm^{-1} K^{-1} from 300 to 550 K; and for a bi-layer, -0.0137 cm^{-1} K^{-1} and -0.0189 cm^{-1} K^{-1} from 300 to 550 K.[24] Apparently, the absolute and relative magnitudes of the temperature coefficients for the two modes differ significantly in these reported values. Furthermore, reliable data for the bulk MoS_2, which may serve as the references, are not readily available in the literature. The intrinsic mechanism for the redshift of the Raman frequency with increasing temperature, as is known for most materials, is associated with the anharmonic effect due to weakening of the lattice potential energy.[25] In our work, we report the temperature dependent Raman measurements of single- and bi-layer MoS_2 in a larger temperature range from 300 to 773 K with small temperature increments, which allows us to accurately examine not only the nonlinearity of the temperature dependence but also the dependence of the film–substrate coupling on the substrate type.

Experimental section

Samples

The samples investigated in this work have been obtained by two methods: mechanical exfoliation and chemical vapor deposition (CVD) as reported in ref. 16. The 1L MoS_2 flake was mechanically exfoliated from nature crystalline bulk MoS_2 and transferred onto a silicon wafer covered by a 300 nm-thick thermal oxide (SiO_2) layer (sample 1L-ME-SiO_2). The CVD-grown 1L and 2L samples were prepared on two types of substrates, SiO_2/Si and sapphire labeled as, respectively, 1L-CVD-SiO_2, 1L-CVD-Sa, 2L-CVD-SiO_2, and 2L-CVD-Sa. Originally the MoS_2 films were grown on sapphire wafers, and then transferred onto SiO_2/Si wafers by Scotch tape. The Raman system used in this work was a Horiba LabRam HR800 with a spectral resolution smaller than 1 cm^{-1}. A 532 nm laser was used with power ~1 mW, low enough to avoid heating of the samples. The temperature dependent measurements were performed with a 50× long-working-distance lens.

Characterization of samples

Fig. 2(a) shows the optical image of an exfoliated 1L MoS_2 film on the SiO_2/Si wafer, with an AFM image in Fig. 2(b), confirming the one-layer thickness which is ~0.7 nm. The Raman frequency difference ($\Delta\omega$) between the E^1_{2g} and A_{1g} modes has been shown to correlate with the layer number, with $\Delta\omega = 19$ cm^{-1} for 1L and 22 cm^{-1} for 2L.[21] Raman mappings of exfoliated films were carried out to examine the thickness distribution of the MoS_2 film at room temperature, and the spatial variation of the frequency difference $\Delta\omega$ is shown in Fig. 2(c). All the $\Delta\omega$ values are found less than 20 cm^{-1}, indicating that it is indeed single-layer MoS_2. Room temperature Raman and photoluminescence (PL) spectra of all the samples, including a bulk MoS_2 sample, used in this work are shown in Fig. 2(d) and (e), respectively. With increasing number of layers, the E^1_{2g} peak shows a redshift in Raman frequency while the A_{1g} peak shows a blueshift. There are small shifts in the peak position among samples of the same thickness but on different substrates, due to residual strain, suggesting some coupling between the film and the substrate. In addition, the line widths of 1L and 2L samples are somewhat larger than those of the bulk sample, which could be an indication of inhomogeneity of the strain. It has been reported that the PL of MoS_2 has two peaks that correspond to A1 (1.85 eV) and B1 (1.98 eV) direct excitonic transitions of MoS_2.[13] The A1 and B1 transitions are, respectively, at 1.82 eV and 1.98 eV for sample 1L-ME-SiO_2, 1.87 eV and 2.0 eV for single-layer CVD samples, and 1.85 eV and 1.99 eV for bi-layer CVD samples. The variation of PL peak positions of MoS_2 samples could be due to the interaction between the film and the substrate and possibly impurities in the films. Additionally, the 1L MoS_2 samples show the strongest PL signal, while bulk MoS_2 negligible, as expected due to the electronic band structure change.

Experimental setup

For the temperature dependent study, a Linkam TS1500 heating system, with a temperature control accuracy of 1 °C, was used to heat the samples with a step of 25 °C, and heating rate of 10 °C min^{-1}. A time of five minutes was applied to hold the temperature at each temperature step, allowing sufficient time for stabilization. An extremely low flow rate of nitrogen gas was

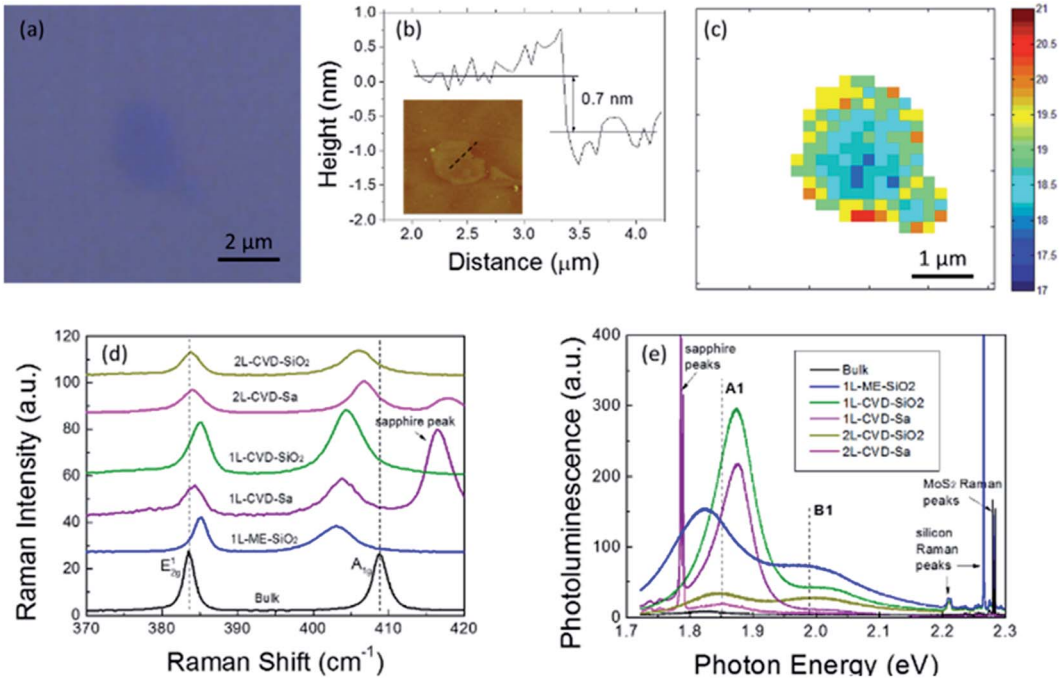

Fig. 2 Optical image (a) and AFM image (b) of the mechanically exfoliated 1L MoS_2 on SiO_2/Si. (c) Map of the Raman frequency difference $\Delta\omega$, and the unit is cm^{-1}. (d) and (e) Raman and PL spectra of bulk MoS_2, and 1L and 2L on different substrates.

purged to avoid the oxidization of MoS_2 to MoO_3. After the sample temperature stabilized, Raman spectra were acquired using the Horiba Raman system. A few samples were heated in the ambient environment, and no Raman signals of E^1_{2g} and A_{1g} modes were observed when the temperature was >350 °C, implying total oxidization of MoS_2 films.

Results and discussion

Temperature dependence of Raman scattering

The temperature dependences of both E^1_{2g} and A_{1g} peak positions were performed in the range from room temperature (25 °C) to 500 °C, as shown in Fig. 3(a)–(d). The upper temperature range in this work is substantially higher than those in the previous studies (< 250 °C).[23,24] The results of bulk MoS_2 are used as a reference. Empirically, the temperature dependence of the Raman shift can be described by:

$$\omega(\Delta T) = \omega_0 + \chi_1\Delta T + \chi_2(\Delta T)^2 + \chi_3(\Delta T)^3, \quad (1)$$

where ω_0 is the frequency at room temperature, ΔT is the temperature change relative to room temperature, and χ_1 is the first-order temperature coefficient. The second (χ_2), third (χ_3) or higher order temperature effects are usually assumed to be small in the literature. In reality, the nonlinear effects are found to be quite significant for 1L or 2L MoS_2 even in a temperature range where the linear dependence might be expected to be adequate, for instance, below 200 °C, depending on the substrate. Even for bulk MoS_2, the nonlinearity occurs at around 200 °C for both E^1_{2g} and A_{1g}, though rather weak, but nevertheless evident in our data. It is perhaps reasonable to assume that the temperature shift for a free standing few-layer MoS_2 should be rather close to that of the bulk material, despite the difference in the absolute position. Therefore, to show more clearly the substrate effect, we can take the temperature shifts of the bulk sample as references. Fig. 3(e)–(h) plot the difference in the Raman frequency shifts between the thin film sample and the bulk, $\delta\omega(\Delta T) = |\omega(\Delta T) - \omega_0|_{\text{thin film}} - |\omega(\Delta T) - \omega_0|_{\text{bulk}}$, for E^1_{2g} and A_{1g} and for 1L and 2L samples. Below we discuss separately E^1_{2g} and A_{1g} to examine the effects of two types of substrates.

(1) E^1_{2g}: for both the 1L and 2L samples, as shown in Fig. 3(a), (c), (e) and (g), the E^1_{2g} mode exhibits relatively weak nonlinearity or in general appears to be close to the temperature dependences of the bulk sample. The temperature dependences of the deviations from the bulk mode are qualitatively similar for the same type of substrate: 1L-CVD-Sa and 2L-CVD-Sa *vs.* 1L-CVD-SiO_2 and 2L-CVD-SiO_2, which is more apparent in Fig. 3(e) and (g), due to subtle difference in the film–substrate coupling (to be discussed later). The deviations of 1L-ME-SiO_2 are somewhat different from the other samples, as shown in Fig. 3(e).

(2) A_{1g}: for both 1L-ME-SiO_2 and 1L-CVD-SiO_2, as shown in Fig. 3(b) and (f), the temperature dependence of A_{1g} mode is drastically different from that of the bulk, showing strong nonlinearity starting at temperatures near 100 °C and an overall S-shape dependence. The Raman spectra of 1L-ME-SiO_2 at a few representative temperatures are shown in Fig. 4. The FWHM of A_{1g} mode is 5.7 cm^{-1} at room temperature, increasing to a maximum of 10.3 cm^{-1} at around 125 °C, then it decreases to 6.3 cm^{-1} when the temperature reaches 500 °C, whereas the FWHM of E^1_{2g} mode increases from 2.2 cm^{-1} at room

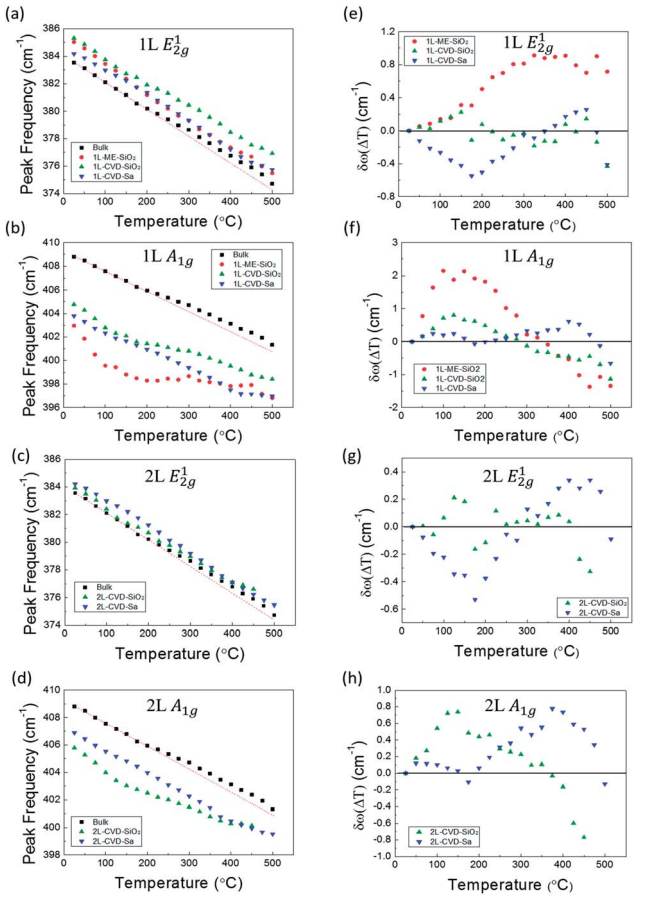

Fig. 3 (a)–(d) Temperature dependence of Raman frequencies of E^1_{2g} and A_{1g} modes in bulk and all other 1L and 2L samples. (e)–(h) The Raman frequency deviation of 1L and 2L MoS_2 relative to bulk MoS_2 as the reference.

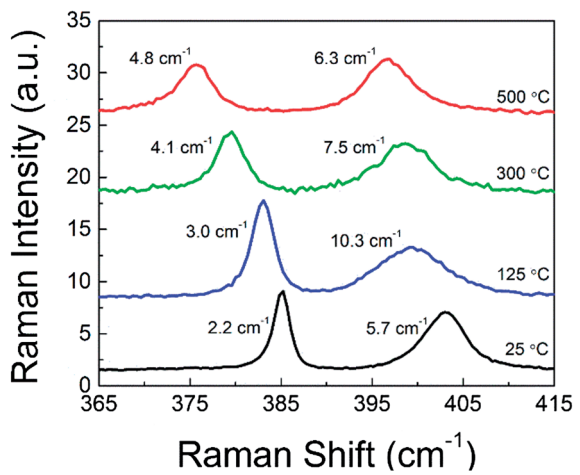

Fig. 4 Representative Raman spectra of the 1L-ME-SiO_2 sample at particular temperatures. The FWHM of E^1_{2g} and A_{1g} are labelled besides the peaks.

temperature monotonically to 4.8 cm^{-1} at 500 °C. However, 1L-CVD-Sa shows only small deviation from the bulk dependence, with an average slope of −0.0159 cm^{-1} K^{-1} by using linear fitting, up to 425 °C, then an obvious change occurs, becoming nearly flat with a slope of −0.0027 cm^{-1} K^{-1}. As for the 2L samples, Fig. 3(d) and (h), similar to 1L-CVD-SiO_2, 2L-CVD-SiO_2 exhibits more significant deviation from the bulk sample than 2L-CVD-Sa when temperature is < 400 °C. For 2L-CVD-Sa, the slope changes significantly when temperature is > 400 °C from −0.0162 cm^{-1} K^{-1} to −0.0102 cm^{-1} K^{-1}. Again, one may notice that the temperature dependences of the deviations from the bulk mode are qualitatively similar for the same type of substrate: 1L-CVD-Sa and 2L-CVD-Sa *vs.* 1L-CVD-SiO_2 and 2L-CVD-SiO_2, which is more apparent in Fig. 3(f) and (h).

Visually from Fig. 3(a)–(d), the A_{1g} mode shows more nonlinearity than the E^1_{2g} mode. Qualitatively similar results have been observed in graphene: the peak position of the G band, an in-plane vibrational mode, is less susceptible to the substrate influence than an out-of-plane vibration mode ~861 cm^{-1}.[26,27] Similarly it is reasonable to expect that in MoS_2 the in-plane mode (E^1_{2g}) will be less affected by the interaction between the film and the substrate than the out-of-plane mode (A_{1g}). Thus, it is not difficult to understand that the E^1_{2g} mode typically shows a more linear temperature dependent Raman shift than A_{1g} mode for both 1L and 2L samples. The difference between the SiO_2 and sapphire substrates also indicates that the coupling between the film and the substrate depends on the substrate type and/or how the film and the substrate are bound.

The temperature coefficients of all the samples are fitted to a third order polynomial function according to eqn (1), and are listed in Table 1. The linear temperature coefficients of E^1_{2g} and A_{1g} in bulk MoS_2 are $\chi_1 = -0.0221 \pm 8.9 \times 10^{-4}$ cm^{-1} K^{-1} and $-0.0197 \pm 8.9 \times 10^{-4}$ cm^{-1} K^{-1}, respectively. Bulk MoS_2, as the reference, can be treated as a stacking of single-layered MoS_2 films, and each layer has the same properties. With increasing temperature, all layers expand with the same rate without introducing any strain, leading to a nearly linear redshift of the Raman peak position for both E^1_{2g} and A_{1g} modes. Although the interlayer coupling has led to significant frequency shifts for the two modes between 1L and bulk, the changes in temperature coefficients are expected to be relatively small. For the E^1_{2g} mode, the first-order temperature coefficients (χ_1) of SiO_2 samples, both 1L and 2L, are close to those of bulk MoS_2, while those of the sapphire samples are much smaller. For A_{1g}, all the SiO_2 samples yield much larger χ_1's than that of bulk MoS_2, while sapphire samples are close to that of bulk MoS_2. Our results for the films on SiO_2/Si are contradicting to or significantly different from those reported in the literature, because the improved data accuracy allows examination of the nonlinear effect that was neglected.[23,24]

Because all the SiO_2 samples were produced by mechanical exfoliation, it is possible that wrinkles or ripples were introduced to the films, resulting in a considerable strain in the film.[28] Fig. 5 shows the spatial maps of the Raman frequencies of E^1_{2g} and A_{1g} modes for the mechanically exfoliated single-layer MoS_2 film on SiO_2/Si (1L-ME-SiO_2) at room temperature. The maps demonstrate that the frequency of A_{1g} shows a larger variation than that of E^1_{2g}, indicating that the morphology of the film impacts the Raman frequency of A_{1g} more than that of E^1_{2g}. On the other hand, both 1L and 2L MoS_2 films were originally grown on sapphire. It has been reported, for graphene, the possibility of forming bonds between

Table 1 Temperature coefficients of bulk, 1L and 2L samples with polynomial fitting to the third order

		χ_1	χ_2	χ_3
E^1_{2g}	Bulk	$-0.0221 \pm 8.9 \times 10^{-4}$	$2.12 \times 10^{-5} \pm 4.4 \times 10^{-6}$	$-2.94 \times 10^{-8} \pm 6.1 \times 10^{-9}$
	1L-ME-SiO_2	-0.0241 ± 0.0015	—	—
	1L-CVD-SiO_2	-0.0217 ± 0.0017	$2.04 \times 10^{-5} \pm 8.4 \times 10^{-6}$	$-2.68 \times 10^{-8} \pm 1.2 \times 10^{-8}$
	1L-CVD-Sa (up to 425 °C)	$-0.0143 \pm 5.7 \times 10^{-4}$	$-1.44 \times 10^{-5} \pm 3.4 \times 10^{-6}$	$7.71 \times 10^{-9} \pm 5.6 \times 10^{-9}$
	2L-CVD-SiO_2 (up to 400 °C)	-0.0233 ± 0.0018	$3.00 \times 10^{-5} \pm 1.1 \times 10^{-5}$	$-4.61 \times 10^{-8} \pm 2.0 \times 10^{-8}$
	2L-CVD-Sa (up to 425 °C)	$-0.0135 \pm 8.4 \times 10^{-4}$	$-2.54 \times 10^{-5} \pm 5.0 \times 10^{-6}$	$2.93 \times 10^{-8} \pm 8.2 \times 10^{-9}$
	1L-ME-SiO_2 (ref. 24)	−0.0179		
	2L-ME-SiO_2 (ref. 24)	−0.0137		
	Few layer (ref. 23)	−0.0132		
A_{1g}	Bulk	$-0.0197 \pm 8.9 \times 10^{-4}$	$2.49 \times 10^{-5} \pm 4.4 \times 10^{-6}$	$-3.53 \times 10^{-8} \pm 6.1 \times 10^{-9}$
	1L-ME-SiO_2	-0.0626 ± 0.0038	$2.11 \times 10^{-4} \pm 1.7 \times 10^{-5}$	$-2.34 \times 10^{-7} \pm 2.1 \times 10^{-8}$
	1L-CVD-SiO_2	-0.0301 ± 0.0023	$8.15 \times 10^{-5} \pm 1.1 \times 10^{-5}$	$-1.00 \times 10^{-7} \pm 1.6 \times 10^{-8}$
	1L-CVD-Sa (up to 425 °C)	-0.0199 ± 0.0012	$3.10 \times 10^{-5} \pm 7.2 \times 10^{-6}$	$-5.77 \times 10^{-8} \pm 1.2 \times 10^{-8}$
	2L-CVD-SiO_2 (up to 400 °C)	-0.0310 ± 0.0018	$8.56 \times 10^{-5} \pm 1.2 \times 10^{-5}$	$-1.16 \times 10^{-7} \pm 2.0 \times 10^{-8}$
	2L-CVD-Sa (up to 425 °C)	-0.0160 ± 0.0014	—	—
	1L-ME-SiO_2 (ref. 24)	−0.0143		
	2L-ME-SiO_2 (ref. 24)	−0.0189		
	Few layer (ref. 23)	−0.0123		

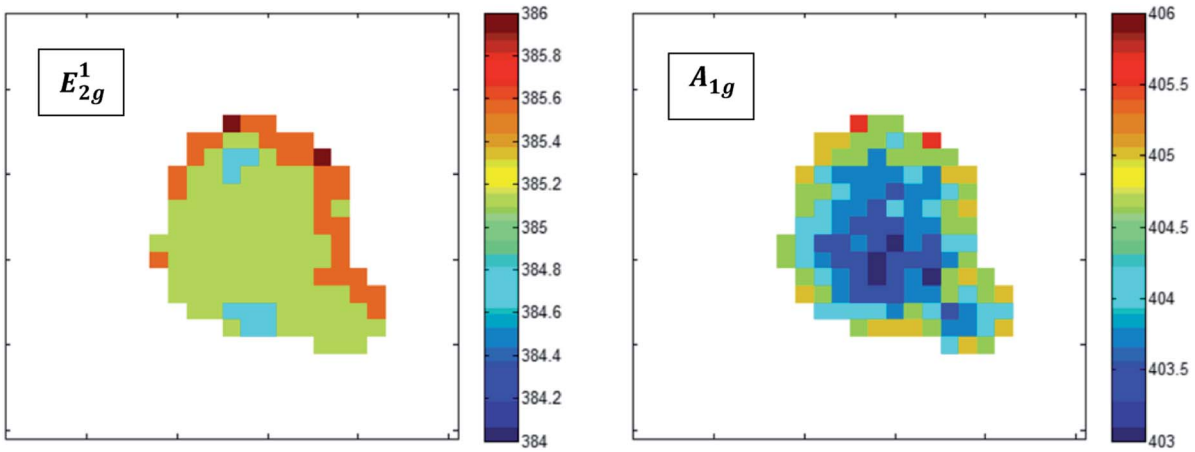

Fig. 5 Spatial maps (6 μm × 6 μm) of the Raman frequencies of (a) E^1_{2g} and (b) A_{1g} modes for the 1L-ME-SiO_2 sample, and the unit is cm^{-1}.

mechanically exfoliated graphene and the substrate is quite low; however, such bonds are possible with high-temperature growth.[29] It is reasonable to believe that the CVD growth of MoS_2 films at a temperature higher than 800 °C could produce somewhat stronger bonding between the MoS_2 film and sapphire substrate than in the case of the transferred film. With increasing temperatures, the chemical bonding would influence the in-plane vibration, giving rise to the damping of the Raman frequency redshift to E^1_{2g} mode in the low temperature region, as manifested on the reduced magnitude of χ_1 for the CVD-grown MoS_2 films on sapphire. Furthermore, the film–substrate coupling leads to the sign changes for both χ_2 and χ_3 compared to the bulk for the E^1_{2g} mode of the on-sapphire samples. In contrast, mechanically transferred MoS_2 films on SiO_2/Si do not form the chemical bonding between the film and the substrate other than the van der Waals force, leading to the temperature dependence of the Raman shift or χ_1 of the E^1_{2g} mode similar to bulk MoS_2. However, the MoS_2 films on SiO_2/Si are more likely to be affected by the changes in the film morphology such as wrinkles and ripples when temperature increases, due to thermal expansion coefficient mismatch between MoS_2 and SiO_2. These changes of morphology in turn will have a large impact on out-of-plane vibration (A_{1g}), causing not only the nonlinear effect of temperature coefficient but also the large deviation of χ_1 from bulk MoS_2 for the SiO_2/Si samples. As for the sapphire samples, the chemical bonding restricts the MoS_2 film from morphology change, and the coupling with the substrate has a relatively small influence on the A_{1g} mode. Therefore, we can conclude that the morphology of MoS_2 films plays a significant role in temperature dependence of A_{1g} mode, which leads to the large and highly non-linear deviation from the bulk, while the bonding between the film and the substrate introduces weaker effects, in similar magnitudes, to both E^1_{2g} and A_{1g} modes on their temperature induced Raman shifts.

The integrated Raman intensity for both E^1_{2g} and A_{1g} modes has been found to decrease in all CVD-grown samples when temperature is > 400 °C, possibly due to the decomposition of MoS_2 films. The thermal decomposition temperature for most samples including bulk is somewhere > 500 °C, except for 2L-CVD-SiO_2 being near 450 °C. For all CVD-grown MoS_2 films on sapphire, no Raman signal is detected when the temperature reaches 575 °C, indicating the decomposition of MoS_2 films. The Raman spectrum does not recover at room temperature after reaching the maximum temperature. The main change is that the frequency difference between A_{1g} and E^1_{2g} modes increases by 2.5 cm^{-1} for 1L-ME-SiO_2. In addition, their peak intensities decrease. There are at least two possible reasons: (1) the strain or morphology has changed, as expected, and (2) the sample might be partially oxidized or decomposed. Similar results have been reported for graphene.[30]

Simulation model for temperature dependence of the Raman shift

The intrinsic temperature dependence of the Raman shift can be divided into thermal expansion of the lattice ($\Delta\omega_E$) and an anharmonic effect ($\Delta\omega_A$) which causes the change of phonon self-energy.[27,31,32] In addition, thermally induced strains due to a thermal expansion coefficient mismatch ($\Delta\omega_M$) between the MoS_2 film and the substrate should be considered.[28] Thus, the measured frequency change can be written as

$$\Delta\omega(T) = \Delta\omega_E(T) + \Delta\omega_A(T) + \Delta\omega_M(T), \quad (2)$$

where T is the sample temperature. Firstly, with increasing temperatures, the lattice constant of the MoS_2 structure increases due to thermal expansion of the film, leading to the Raman shift which is commonly expressed as[32]

$$\Delta\omega_E(T) = \omega_0 \exp\left(-n\gamma\int_{25^\circ C}^{T}\alpha dT\right) - \omega_0, \quad (3)$$

where ω_0 is the room temperature frequency, n is the degeneracy, 1 for A_{1g} mode and 2 for E^1_{2g} mode, γ is the Grüneisen parameter, and α is the thermal expansion coefficient of the material. The Grüneisen parameters of both E^1_{2g} and A_{1g} modes for bulk MoS_2 are $\gamma(E^1_{2g}) = 0.21$ and $\gamma(A_{1g}) = 0.42$, respectively. The in-plane and out-of-plane thermal expansion coefficients for bulk MoS_2 have been derived from the results of ref. 33:

$$\alpha_a(T) = \left(\frac{0.6007\times10^{-5} + 0.6958\times10^{-7}T}{a}\right)\left(\frac{1}{^\circ C}\right)$$
$$\alpha_c(T) = \left(\frac{0.1064\times10^{-3} + 1.5474\times10^{-7}T}{c}\right)\left(\frac{1}{^\circ C}\right), \quad (4)$$

where T is the temperature in °C, a and c are the lattice constants of MoS_2 in Å. They are calculated to be 2.48 × 10^{-6} $^\circ C^{-1}$ and 9.14 × 10^{-6} $^\circ C^{-1}$, respectively, for in-plane and out-of-plane thermal expansion coefficients at room temperature. The second term of the right-hand side in eqn (2) is related to a pure temperature effect, so-called "self-energy" shift due to anharmonic coupling of multiple phonons, which can be written as[31]

$$\Delta\omega_A(T) = A\left(1 + \frac{2}{e^x - 1}\right) + B\left(1 + \frac{3}{e^y - 1} + \frac{3}{(e^y - 1)^2}\right), \quad (5)$$

where $x = \hbar\omega/2kT$, $y = \hbar\omega/3kT$, and the first term corresponds to coupling of the optical phonon to two identical phonons, and the second term represents the coupling to three identical phonons. The coefficients A and B are constants that can be estimated by fitting the frequency shift attributes to anharmonic coupling. The possible remaining change of the Raman shift is associated with the thermal expansion coefficient mismatch between the film and the substrate, introducing strain to the film, which can be expressed as[28]

$$\Delta\omega_M(T) = \beta\int_{25^\circ C}^{T}\left(\alpha_{sub}(T) - \alpha_{MoS_2}(T)\right)dT, \quad (6)$$

where β is the biaxial strain coefficient, α_{sub} and α_{MoS_2} are the thermal expansion coefficients of the substrate and MoS_2, respectively. For bulk MoS_2, there is no thermal expansion coefficient mismatch between MoS_2 layers, so that the third term is zero. Eqn (6) assumes that the film and the substrate are in coherent strain, which is likely invalid for the transferred film. Fig. 6 shows these contributions to the changes in Raman peak positions of both E^1_{2g} and A_{1g} modes for bulk MoS_2 with good agreement with experimental results. Table 2 shows the fitting parameters of A and B for both E^1_{2g} and A_{1g} modes.

However, this model, which predicts monotonic behavior, is not appropriate for MoS_2 films, either 1L or 2L, on substrates. In the case of MoS_2 films on substrates like SiO_2/Si and sapphire, according to eqn (6) with β being −2.1 cm^{-1} per % strain, the contribution of the thermal expansion coefficient mismatch is expected to be negligible compared to the thermal expansion of the lattice and anharmonic effect in the temperature region of interest.[34,35] With increasing temperatures, the biaxial tensile or compressive strain induced by the thermal expansion coefficient mismatch increases significantly over the van der Waals force, resulting in the slippage or realignment of MoS_2 films on the surface of the substrate as well as forming wrinkles or ripples. For the 1L-ME-SiO_2 sample, the realignment process takes place at ~100 °C where there is an obvious slope transition of the A_{1g} peak position. During the realignment process, defects may be introduced into the MoS_2 film such as the breakdown of Mo–S bonds and the slow decomposition of the film, showing a broadening of

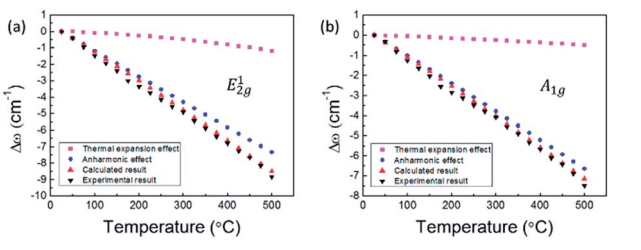

Fig. 6 The model of a temperature dependent Raman shift relative to room temperature including the contributions of a thermal expansion effect of the lattice and anharmonic effect as compared to experimental results of bulk MoS_2 for (a) E^1_{2g} and (b) A_{1g} modes.

Table 2 The fitting parameters A and B for both E^1_{2g} and A_{1g} modes used in the three- and four-phonon coupling model

Bulk MoS_2	A (cm^{-1})	B (cm^{-1})
E^1_{2g}	−3.05835	0.04204
A_{1g}	−5.68777	0.26566

the A_{1g} Raman peak (Fig. 4). After the MoS_2 layer adjusts to a stable state on the SiO_2/Si substrate at high temperature, the Raman shift of the A_{1g} mode again follows what is expected from eqn (2).

Full width at half maximum (FWHM)

Fig. 7 shows the temperature dependent FWHM of both E^1_{2g} peak and A_{1g} peak for all samples, by fitting to a Lorentzian lineshape function. Bulk MoS_2 has room-temperature FWHMs of 1.6 cm^{-1} and 2.2 cm^{-1}, respectively, for E^1_{2g} and A_{1g}. Other samples have greater FWHMs, indicating that the film–substrate coupling and defects existing in these samples cause peak broadening. The FWHM of the E^1_{2g} mode, in general, increases linearly with increasing temperatures. However, the A_{1g} mode does not show a monotonic dependence but with a maximum linewidth in the middle of the temperature range. As it is discussed above, the mismatch of thermal expansion coefficients between MoS_2 films and substrates gives rise to changes of morphology *e.g.* wrinkles or ripples, consequently leading to a significant change of the temperature coefficients of the A_{1g} mode. For all 1L and 2L samples, the FWHM of A_{1g} reaches the maximum when the realignment process occurs. For instance, the anomaly of the temperature dependent Raman shift of 1L-ME-SiO_2 takes places at the temperatures starting from ~100 °C, while the FWHM reaches the maximum at 125 °C and then starts to decrease afterward. This gives an additional illustration that the change of the morphology by the thermal expansion coefficient mismatch can affect the out-of-plane vibrational mode more than the in-plane mode when the temperature reaches a critical value.

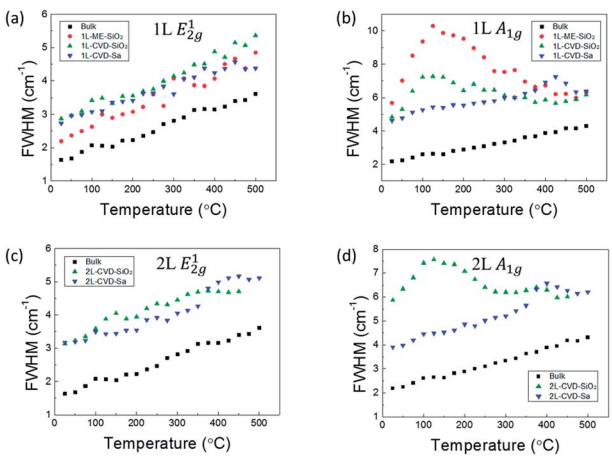

Fig. 7 Temperature dependence of FWHM of E^1_{2g} and A_{1g} modes in bulk and all other 1L and 2L samples.

Conclusions

In summary, we have reported temperature-dependent Raman studies of the in-plane E^1_{2g} and out-of-plane A_{1g} modes on single- and bi-layer MoS_2 samples prepared by CVD growth and mechanical exfoliation on SiO_2/Si and sapphire substrates in the temperature range of 25–500 °C. Bulk MoS_2 has also been measured to serve as the references, with the first-order temperature coefficients of the Raman frequency shifts given as $\chi_1(E^1_{2g}) = -0.0221 \pm 8.9 \times 10^{-4}$ cm^{-1} K^{-1} and $\chi_1(A_{1g}) = -0.0197 \pm 8.9 \times 10^{-4}$ cm^{-1} K^{-1}, respectively, for the E^1_{2g} and A_{1g} modes. The thermal decomposition temperature is found to be approximately 575 °C for CVD-grown films on sapphire. The film–substrate coupling affects the temperature dependence of Raman frequency, intensity, and linewidth for both E^1_{2g} and A_{1g} modes in the 1L and 2L MoS_2. The impact depends on the substrate type and/or film–substrate binding mechanism. For the CVD grown film on the original sapphire substrate with likely chemical bonding between them, the film–substrate coupling significantly reduces the linear temperature coefficients of the Raman shift of the E^1_{2g} mode to $-0.0143 \pm 5.7 \times 10^{-4}$ cm^{-1} K^{-1} for the 1L and $-0.0135 \pm 8.4 \times 10^{-4}$ cm^{-1} K^{-1} for the 2L, but has no or small effect on the A_{1g} mode, with -0.0199 ± 0.0012 cm^{-1} K^{-1} for the 1L and -0.0160 ± 0.0014 cm^{-1} K^{-1} for the 2L. For the transferred film on the SiO_2/Si substrate, originally grown on sapphire by CVD, for the E^1_{2g} mode, the temperature coefficients were found to be very close to the bulk value as -0.0217 ± 0.0017 cm^{-1} K^{-1} for the 1L and -0.0233 ± 0.0018 cm^{-1} K^{-1} for the 2L; but for the A_{1g} mode, they increase substantially to -0.0301 ± 0.0023 cm^{-1} K^{-1} for the 1L and -0.0310 ± 0.0018 cm^{-1} K^{-1} for the 2L. The substrate effects are most pronounced for the A_{1g} mode, showing as stronger nonlinearity on the temperature shift of the Raman frequency and non-monotonic temperature dependence of the Raman linewidth. Similar or even stronger effects were observed on a mechanically exfoliated 1L film from a bulk single crystal. These results suggest that for the mechanically transferred thin film, due to the mismatch in thermal expansion between the film and substrate, the temperature change can lead to significant changes in the thin-film morphology as a result of realignment of the film on the substrate, which can be most easily probed by the temperature dependence of the A_{1g} mode associated with the out-of-plane atomic vibration. Temperature dependent Raman study provides an efficient tool for investigating the coupling between the 2-D material and the substrate either with chemical or mechanical bonding.

Note added in proof

After the acceptance of this paper, it was brought to our attention that the temperature coefficients for the E^1_{2g} and A_{1g} modes in bulk 2H-MoS_2 were reported to be, respectively, -1.47×10^{-2}

cm^{-1} K^{-1} and -1.23×10^{-2} cm^{-1} K^{-1} in the following reference: T. Livneh and E. Sterer, *Phys. Rev. B*, 2010, **81**, 195209.

Acknowledgements

Y.Z. acknowledges the support of Bissell Distinguished Professorship. L.C. acknowledges the support of a Young Investigator Award from the Army Research Office (W911NF-13-1-0201).

Notes and references

1 K. S. Novoselov, A. K. Geim, S. V. Morozov, D. Jiang, M. I. Katsnelson, I. V. Grigorieva, S. V. Dubonos and A. A. Firsov, *Nature*, 2005, **438**, 197–200.
2 Y.-M. Lin, C. Dimitrakopoulos, K. A. Jenkins, D. B. Farmer, H.-Y. Chiu, A. Grill and P. Avouris, *Science*, 2010, **327**, 662.
3 F. Schwierz, *Nat. Nanotechnol.*, 2010, **5**, 487–496.
4 K. S. Novoselov, A. K. Geim, S. V. Morozov, D. Jiang, Y. Zhang, S. V. Dubonos, I. V. Grigorieva and A. A. Firsov, *Science*, 2004, **306**, 666–669.
5 K. Watanabe, T. Taniguchi and H. Kanda, *Nat. Mater.*, 2004, **3**, 404–409.
6 C. Jin, F. Lin, K. Suenaga and S. Iijima, *Phys. Rev. Lett.*, 2009, **102**, 195505.
7 I. Meric, M. Y. Han, A. F. Young, B. Ozyilmaz, P. Kim and K. L. Shepard, *Nat. Nanotechnol.*, 2008, **3**, 654–659.
8 Y.-W. Son, M. L. Cohen and S. G. Louie, *Phys. Rev. Lett.*, 2006, **97**, 216803.
9 G. Giovannetti, P. A. Khomyakov, G. Brocks, P. J. Kelly and J. van den Brink, *Phys. Rev. B: Condens. Matter Mater. Phys.*, 2007, **76**, 073103.
10 Y. Zhang, T.-T. Tang, C. Girit, Z. Hao, M. C. Martin, A. Zettl, M. F. Crommie, Y. R. Shen and F. Wang, *Nature*, 2009, **459**, 820–823.
11 Y. Kubota, K. Watanabe, O. Tsuda and T. Taniguchi, *Science*, 2007, **317**, 932–934.
12 K. F. Mak, C. Lee, J. Hone, J. Shan and T. F. Heinz, *Phys. Rev. Lett.*, 2010, **105**, 136805.
13 A. Splendiani, L. Sun, Y. Zhang, T. Li, J. Kim, C.-Y. Chim, G. Galli and F. Wang, *Nano Lett.*, 2010, **10**, 1271–1275.
14 B. Radisavljevic, A. Radenovic, J. Brivio, V. Giacometti and A. Kis, *Nat. Nanotechnol.*, 2011, **6**, 147–150.
15 Y. Zhan, Z. Liu, S. Najmaei, P. M. Ajayan and J. Lou, *Small*, 2012, **8**, 966–971.
16 Y. Yu, C. Li, Y. Liu, L. Su, Y. Zhang and L. Cao, *Sci. Rep.*, 2013, 3.
17 A. Molina-Sánchez and L. Wirtz, *Phys. Rev. B: Condens. Matter Mater. Phys.*, 2011, **84**, 155413.
18 E. S. Kadantsev and P. Hawrylak, *Solid State Commun.*, 2012, **152**, 909–913.
19 X. Zhang, W. P. Han, J. B. Wu, S. Milana, Y. Lu, Q. Q. Li, A. C. Ferrari and P. H. Tan, *Phys. Rev. B: Condens. Matter Mater. Phys.*, 2013, **87**, 115413.
20 M. Ghorbani-Asl, N. Zibouche, M. Wahiduzzaman, A. F. Oliveira, A. Kuc and T. Heine, *Sci. Rep.*, 2013, 3.
21 H. Li, Q. Zhang, C. C. R. Yap, B. K. Tay, T. H. T. Edwin, A. Olivier and D. Baillargeat, *Adv. Funct. Mater.*, 2012, **22**, 1385–1390.
22 A. C. Ferrari, J. C. Meyer, V. Scardaci, C. Casiraghi, M. Lazzeri, F. Mauri, S. Piscanec, D. Jiang, K. S. Novoselov, S. Roth and A. K. Geim, *Phys. Rev. Lett.*, 2006, **97**, 187401.
23 S. Sahoo, A. P. S. Gaur, M. Ahmadi, M. J. F. Guinel and R. S. Katiyar, *J. Phys. Chem. C*, 2013, **117**, 9042–9047.
24 S. Najmaei, P. M. Ajayan and J. Lou, *Nanoscale*, 2013, **5**, 9758–9763.
25 P. G. Klemens, *Phys. Rev.*, 1966, **148**, 845–848.
26 L. A. Falkovsky, *J. Exp. Theor. Phys.*, 2007, **105**, 397–403.
27 I. Calizo, A. A. Balandin, W. Bao, F. Miao and C. N. Lau, *Nano Lett.*, 2007, **7**, 2645–2649.
28 D. Yoon, Y.-W. Son and H. Cheong, *Nano Lett.*, 2011, **11**, 3227–3231.
29 Y. Y. Wang, Z. H. Ni, T. Yu, Z. X. Shen, H. M. Wang, Y. H. Wu, W. Chen and A. T. Shen Wee, *J. Phys. Chem. C*, 2008, **112**, 10637–10640.
30 Z. H. Ni, H. M. Wang, Z. Q. Luo, Y. Y. Wang, T. Yu, Y. H. Wu and Z. X. Shen, *J. Raman Spectrosc.*, 2010, **41**, 479–483.
31 M. Balkanski, R. F. Wallis and E. Haro, *Phys. Rev. B: Condens. Matter Mater. Phys.*, 1983, **28**, 1928–1934.
32 J. Menéndez and M. Cardona, *Phys. Rev. B: Condens. Matter Mater. Phys.*, 1984, **29**, 2051–2059.
33 S. H. El-Mahalawy and B. L. Evans, *J. Appl. Crystallogr.*, 1976, **9**, 403–406.
34 H. Tada, A. E. Kumpel, R. E. Lathrop, J. B. Slanina, P. Nieva, P. Zavracky, I. N. Miaoulis and P. Y. Wong, *J. Appl. Phys.*, 2000, **87**, 4189–4193.
35 C. Rice, R. J. Young, R. Zan, U. Bangert, D. Wolverson, T. Georgiou, R. Jalil and K. S. Novoselov, *Phys. Rev. B: Condens. Matter Mater. Phys.*, 2013, **87**, 081307.